Available online at www.sciencedirect.com
SCIENCE DIRECT
ELSEVIER
International Journal of Solids and Structures 43 (2006) 1857–1877
INTERNATIONAL JOURNAL OF SOLIDS and STRUCTURES
www.elsevier.com/locate/ijsolstr

An evaluation of higher-order plasticity theories for predicting size effects and localisation

R.A.B. Engelen [a,c], N.A. Fleck [b], R.H.J. Peerlings [c,*], M.G.D. Geers [c]

[a] Netherlands Institute for Metals Research, P.O. Box 5008, 2600 GA Delft, The Netherlands
[b] Department of Engineering, University of Cambridge, Trumpington Street, Cambridge CB2 1PZ, United Kingdom
[c] Department of Mechanical Engineering, Eindhoven University of Technology, P.O. Box 513, 5600 MB Eindhoven, The Netherlands

Available online 19 January 2006

Abstract

Conventional plasticity theories are unable to capture the observed increase in strength of metallic structures with diminishing size. They also give rise to ill-posed boundary value problems at the onset of material softening. In order to overcome both deficiencies, a range of higher-order plasticity theories have been formulated in the literature. The purpose of this paper is to compare existing higher-order theories for the prediction of a size effect and the handling of localisation effects. To this end, size effect predictions for foils in bending are compared with existing experimental data. Furthermore, a study of one-dimensional harmonic incremental solutions from a uniform reference state allows one to assess the nature of material localisation as predicted by these competing higher-order theories. These analyses show that only one of the theories considered—the Fleck–Hutchinson strain gradient plasticity theory based upon the Toupin–Mindlin strain gradient framework [Fleck, N.A., Hutchinson, J.W., 1997. Strain gradient plasticity. Adv. Appl. Mech. 33, 295–361—allows one to describe both phenomena. The other theories show either nonphysical size effects or a pathologically localised post-peak response.

Keywords: Higher-order continua; Strain gradient plasticity; Nonlocality; Size effects; Softening; Localisation

1. Introduction

Over the past few decades intensive research has been conducted on the development and application of higher-order plasticity theories. The need for these higher-order formulations originates from the inability of the classical plasticity framework to account for observed size effects in plasticity. These effects usually manifest themselves as an increase of the apparent flow strength with diminishing size of specimen or structure when the length scale is on the order of microns. For example, the indentation hardness of metals and ceramics

* Corresponding author. Tel.: +31 40 247 2788; fax: +31 40 244 7355.
E-mail address: R.H.J.Peerlings@tue.nl (R.H.J. Peerlings).

0020-7683/$ - see front matter © 2005 Elsevier Ltd. All rights reserved.
doi:10.1016/j.ijsolstr.2004.05.072

increases with diminishing indenter size for micron-size indents (Ma and Clarke, 1995; Poole et al., 1996; Begley and Hutchinson, 1998). Micro-torsion tests on copper wires show that the inferred shear strength increases with decreasing radius (Fleck et al., 1994). Micro-bending tests on high-purity nickel reveal that the material strength increases with decreasing foil thickness (Stölken and Evans, 1998). Classical plasticity formulations do not contain a material length scale, and so their predictions are independent of the size of the structure.

Discrete dislocation simulations further support the notion of a material length scale: calculations have been performed recently of a constrained layer subjected to simple shear (Shu et al., 2001). The glide of dislocations out of the top and bottom faces of the layer is blocked by an elastic coating, and consequently a boundary layer emerges of reduced plastic slip. Phenomenological plasticity laws are only able to predict such boundary layers when a higher-order formulation is invoked, which allows one to impose additional boundary conditions such as the enforcement of vanishing slip on the constrained faces of the strip.

The experiments on size effects and discrete dislocation simulations indicate that plasticity laws should include a material length scale on the order of microns. A natural way to incorporate such a length scale into the constitutive law is to postulate that the yield strength depends upon both strain and strain gradient. When the length scale associated with the deformation field is comparable to the material length scale, the strain gradient contributes significantly to the yield strength.

Two sources of strain gradient strengthening may be identified within a plastically deforming solid: strengthening due to the formation of a boundary layer at a constrained boundary, such as the strip in shear, and strengthening due to strain gradients in inhomogeneous plastic flow in the bulk of the solid. In both instances the generation of geometrically necessary dislocations, resulting in significant internal stresses as well as short-range interactions with mobile dislocations, gives rise to an increase in flow strength. The physical basis of strain gradient strengthening is discussed further in Fleck and Hutchinson (1993).

A material length scale also emerges in the development of shear bands and fracture. In a shear band the deformation is localised within a confined region as a result of strain softening or strain-rate softening. The thickness of the shear band is finite and is set by the microstructure of the material. In general, this length scale may be different from that associated with the size effect. Standard plasticity models cannot describe the localisation of plastic deformation in a finite band because they lack a length scale which sets the width of the shear band. Indeed, the presence of material softening leads to ill-posed boundary value problems in conventional continua (Benallal et al., 1989; de Borst et al., 1993).

A generally applicable remedy is to incorporate higher-order strain gradients within the constitutive framework. The higher-order theories provide a length scale that sets the shear band width and provide well-posed boundary value formulations (Aifantis, 1984; Coleman and Hodgdon, 1985). Note that another size effect emerges in the localisation (post peak) regime, since the collapse response depends upon the ratio of shear band width (set by the material length scale) and the size of the overall structure. The reader is referred to Bažant (2000) for a full discussion of this topic.

The purpose of the present paper is to review a number of recently developed higher-order theories in order to assess their ability to predict size effects *and* to handle localisation events. Our interest in theories which perform well in both aspects is not only academic, but is also motivated by the miniaturisation trend which can be observed for many components and manufacturing processes. Reliable failure predictions on the micron-scale require theories which are scale-sensitive and which can describe localised plastic flow and damage. Here the size effect for a beam in bending and the one-dimensional localisation for a bar in tension are addressed as prototype problems for a representative set of gradient theories. For the purpose of comparing different formulations, the material length scales in each of the theories are taken to be the same. Furthermore, we neglect elasticity where possible in order to model behaviour deep in the plastic range, where the physical origin of the relevant effects is the most prominent.

Section 2 gives a brief overview of the three higher-order plasticity theories which will be considered in this paper. In each case, conventional von Mises plasticity is recovered when the internal material length scale is set to zero. The following sections are devoted to a study of the size effects predicted by these theories (Section 3) and their ability to handle softening material behaviour (Section 4). Based on the insight acquired in these analyses, conclusions on the capability of these formulations to describe both size effects and localisation events are drawn in Section 5.

2. Review of higher-order plasticity theories

Before embarking on our study of size effects and localisation behaviour, the higher-order plasticity theories which we consider will be briefly reviewed. It is emphasised that many more theories can be found in the literature, but the theories considered here form a representative subset. In particular, gradient theories with and without higher-order stresses are considered, as well as strongly and weakly nonlocal theories. Where relevant, the flow theory versions will be used, but strains and rotations are assumed to be small so that finite strain effects can be neglected.

2.1. Fleck–Hutchinson 1997 strain gradient plasticity

The strain gradient plasticity theory presented in its full form by Fleck and Hutchinson in 1997 is an extension of the Toupin–Mindlin higher-order framework (Toupin, 1962; Mindlin, 1964, 1965) into the plasticity regime. It was developed in order to explain experimentally observed size effects in plastic yielding. The full theory and simpler versions of it have been used to fit such effects in e.g. torsion of thin wires, bending of foils and micro-indentation (Fleck and Hutchinson, 1993, 1997; Fleck et al., 1994; Stölken and Evans, 1998). A preliminary analysis of shear localisation using this theory is given by Fleck and Hutchinson (1998).

The kinematics of the theory take into account the usual first-order gradient of the displacements in the form of the symmetric strain tensor

$$\varepsilon_{ij} = \frac{1}{2}(u_{i,j} + u_{j,i}) \tag{1}$$

(where $i, j = 1, 2, 3$ and a comma indicates partial differentiation) as well as the second-order displacement gradient

$$\eta_{ijk} = u_{k,ij} \tag{2}$$

An earlier version considers only the rotational part of the second-order displacement gradient, leading to a couple-stress theory (Fleck and Hutchinson, 1993). Here, we need to use the full gradient theory, including stretch gradients, because no rotations are present in the one-dimensional localisation study presented in Section 4.

Still following the Toupin–Mindlin strategy, a second-order stress tensor σ_{ij} and a third-order, 'double stress' tensor τ_{ijk} are introduced as work-conjugate quantities to ε_{ij} and η_{ijk} respectively. These stresses must satisfy the higher-order equilibrium equations

$$\sigma_{ik,i} - \tau_{ijk,ij} = 0 \tag{3}$$

where body forces have been neglected.

In addition to appearing in the equilibrium equations, the higher-order stresses also contribute to the surface tractions, which read (Fleck and Hutchinson, 1997)

$$T_k = n_i\sigma_{ik} - n_i\tau_{ijk,j} + n_i n_j \tau_{ijk} D_q n_q - D_j(n_i\tau_{ijk}) \tag{4}$$

Here, n_i is the outward unit normal to the surface and the surface gradient operator D_i is defined as $D_i = (\delta_{ij} - n_i n_j)\partial/\partial x_j$. Note that in a standard continuum only the first term in expression (4) is present. The traction given by (4) is work conjugate to the boundary displacement u_k in the usual way. In addition to this standard surface traction, a 'double-stress' traction t_k must be defined, which is conjugate to the normal displacement gradient on the boundary $u_{k,q}n_q$. This higher-order traction is related to the double stress τ_{ijk} by

$$t_k = n_i n_j \tau_{ijk} \tag{5}$$

When the surface of the body contains edges an additional line load appears, see Fleck and Hutchinson (1997) for details.

Plasticity is introduced by assuming an additive split of both ε_{ij} and η_{ijk} into elastic and plastic parts. The elastic deformation and stress measures are related through an assumed elastic strain energy density

(cf. Toupin, 1962; Mindlin, 1964, 1965). The elastic limit is given by a yield criterion defined in the generalised stress space spanned by σ_{ij} and τ_{ijk}:

$$\Phi = \Sigma(\sigma_{ij}, \tau_{ijk}) - \sigma_{\mathrm{y}}(E_{\mathrm{p}}) \leqslant 0 \tag{6}$$

In this relation Σ is a nonstandard effective stress, and is taken by Fleck and Hutchinson to be a function of σ_{ij} and τ_{ijk} (Fleck and Hutchinson, 1997). The current yield strength σ_{y} depends upon an accumulated effective plastic strain E_{p}, and this is obtained by time integration of an overall effective plastic strain rate $\dot{E}_{\mathrm{p}}$. The overall effective plastic strain rate is defined in terms of the plastic deformation rates $\dot{\varepsilon}^{\mathrm{p}}_{ij}$ and $\dot{\eta}^{\mathrm{p}}_{ijk}$. In the most general form of the isotropic theory, the definitions of Σ and $\dot{E}_{\mathrm{p}}$ feature three separate length scales. In the limiting case of uniform fields the influence of these length scales vanishes and the generalised quantities reduce to the standard von Mises stress and effective plastic strain. Alternatively, when strain gradients are large the overall effective strain is enhanced, and increased hardening results. Plastic flow is assumed to be normal to the yield surface in the extended stress space of σ_{ij} and τ_{ijk}.

2.2. Fleck–Hutchinson 2001 strain gradient plasticity

A second strain gradient plasticity theory was proposed by Fleck and Hutchinson in 2001 in order to reduce the complexity of the modelling, while preserving the ability to predict size effects. Inspired by earlier work of Aifantis, Mühlhaus, de Borst and co-workers (Aifantis, 1984; Mühlhaus and Aifantis, 1991; de Borst and Mühlhaus, 1992), the simplified model considers only gradients of the effective plastic strain rather than gradients of the complete strain tensor. Note that this also implies that gradient effects in the elastic regime are neglected. Furthermore, the standard flow rule is assumed to be valid. A vectorial higher-order stress τ_i is assumed as work conjugate to the effective plastic strain gradient $\varepsilon_{\mathrm{p},i}$. Inserting this extra contribution into the virtual work statement yields the standard equilibrium equation

$$\sigma_{ij,i} = 0 \tag{7}$$

and an additional, scalar equation in terms of the higher-order stress which reads

$$Q = \sigma_{\mathrm{e}} + \tau_{i,i} \tag{8}$$

where Q is defined as the work conjugate to ε_{p} and σ_{e} is the usual von Mises equivalent stress. The yield condition reads $Q \leqslant Q_{\mathrm{y}}(E_{\mathrm{p}})$, where the generalised yield stress Q_{y} is a function of a generalised effective plastic strain E_{p} defined in a similar fashion as in the 1997 Fleck–Hutchinson theory.

Associated with the field equations (7) and (8) are the standard displacement/traction boundary conditions plus a condition in terms of the effective plastic strain or the scalar higher-order traction $t = n_i\tau_i$. The latter, nonstandard condition must be applied at the elastic–plastic boundary and at that portion of the external boundary which has yielded. Note that this is different from the Fleck–Hutchinson 1997 theory, where the additional boundary conditions are always imposed at the external boundary. This difference with the previous theory arises as a consequence of neglecting higher-order contributions to the elastic behaviour in the Fleck–Hutchinson 2001 theory. Free boundaries and internal plastic boundaries are usually assumed not to be able to generate a higher-order traction, so that $t = 0$ is usually employed. Physically, this means at external boundaries that dislocations can freely move out of the material. If dislocation movement is obstructed, for instance by the presence of a hard coating, a more appropriate boundary condition is $\varepsilon_{\mathrm{p}} = 0$ (Fleck and Hutchinson, 2001).

Evolution relations have been derived for Q_{y} and τ_i in the plastic regime:

$$\dot{Q}_{\mathrm{y}} = h(E_{\mathrm{p}})\left(\dot{\varepsilon}_{\mathrm{p}} + \frac{1}{2}B_i\dot{\varepsilon}_{\mathrm{p},i} + C\dot{\varepsilon}_{\mathrm{p}}\right) \tag{9}$$

$$\dot{\tau}_i = h(E_{\mathrm{p}})\left(A_{ij}\dot{\varepsilon}_{\mathrm{p},j} + \frac{1}{2}B_i\dot{\varepsilon}_{\mathrm{p}}\right) \tag{10}$$

with h the usual hardening variable, which is considered to be a function of a generalised effective plastic strain E_{p}. The factors A_{ij}, B_i and C depend on the flow direction and on three independent length parameters, see Fleck and Hutchinson (2001) for details.

If A_{ij}, B_i and C are set to $A_{ij} = \delta_{ij} l^2$, $B_i = C = 0$, with l the single remaining length parameter, the equivalent stress rate can be rewritten in the plastic regime as

$$\dot{\sigma}_e = h(E_p)\dot{\varepsilon}_p - \left(h(E_p) l^2 \dot{\varepsilon}_{p,i}\right)_{,i} \tag{11}$$

This expression is very similar to the one originally proposed by Aifantis (1984) and used later by others (Mühlhaus and Aifantis, 1991; de Borst and Mühlhaus, 1992). Indeed, for constant h it reduces to the expression used by these authors, except for the absence of an influence of the first gradient of ε_p, which is used in some of the work of Aifantis and co-workers. In the following the Fleck and Hutchinson 2001 theory is taken as representative of a wider class of theories which use gradients of the effective plastic strain, but which are based upon the standard equilibrium equation (7).

2.3. Nonlocal plasticity

Nonlocal theories use nonstandard measures of plastic strain in order to introduce spatial interactions at a certain length scale. These interactions are strongly nonlocal, i.e. they act over finite distances, unlike the infinitesimal distances implied by including only gradients of plastic strain or total strain. This appears to be particularly important when modelling fracture, where strong nonlocality is needed to deal with the singularities at a crack tip (Peerlings et al., 2002).

Most nonlocal plasticity theories have been developed for the purpose of regularising localisation of deformation as a result of material softening. The link between nonlocality and regularisation was first made by Bažant, Pijaudier-Cabot and co-workers (Bažant et al., 1984; Pijaudier-Cabot and Bažant, 1987). Most of their developments were done in a continuum damage context, in which they proposed to replace the variable which controls damage growth by a moving, weighted average of this variable in order to smear out damage growth and thus avoid pathological localisation. Following this principle, nonlocal plasticity theories have been proposed, among others, by Leblond et al. (1994), Strömberg and Ristinmaa (1996), Needleman and Tvergaard (1998) and Polizzotto et al. (1998).

Nonlocal models of the above integral type lead to a set of integro-differential equations, which do not fit very well into the numerical solution strategies commonly used in solid mechanics. It has been realised more recently, however, that very similar properties can be obtained by replacing the integral averaging by a partial differential equation. If this differential approximation is chosen properly, the strongly nonlocal character of the integral formulation is preserved (Peerlings et al., 2001). In the damage mechanics context such a formulation was first developed by Peerlings et al. (1996). A coupled damage-plasticity formulation of this type has been developed by Engelen et al. (1999, 2003). A large-strain version of the latter theory has recently been published (Geers et al., 2003). All of these theories aim at regularising localisation of deformation due to strain softening; we have not been able to trace any applications to size effects in hardening.

In this study, we will take the small-strain theory of Engelen et al. (1999, 2003) as representative of the class of nonlocal models. As in the Fleck–Hutchinson 2001 theory, it uses the standard equilibrium equation and the standard flow rule. The yield condition, however, is nonstandard and reads in a general form as

$$\sigma_e \leqslant \sigma_y(\varepsilon_p, \bar{\varepsilon}_p) \tag{12}$$

where ε_p denotes the usual effective plastic strain and $\bar{\varepsilon}_p$ is a nonlocal effective plastic strain. The original theory of Engelen et al. (1999, 2003) was aimed at describing the influence of ductile damage on the flow behaviour of metal alloys. The nonlocal effective strain therefore enters the yield stress via a damage variable, which degrades the undamaged hardening behaviour in a multiplicative way. In order to also have a gradient influence on the undamaged hardening regime, the yield condition has been generalised here to (12).

The nonlocal effective plastic strain $\bar{\varepsilon}_p$ follows from an additional partial differential equation

$$\bar{\varepsilon}_p - l^2 \bar{\varepsilon}_{p,ii} = \varepsilon_p \tag{13}$$

and an associated boundary condition, which is usually defined as

$$n_i \bar{\varepsilon}_{p,i} = 0 \tag{14}$$

The length parameter l in (13) represents the scale at which the nonlocal interactions take place. As in the Fleck–Hutchinson 2001 theory, (13) is coupled with the equilibrium equations. An important difference, however, is that (13) is valid over the entire domain, rather than only in the plastic zone, and the above boundary condition must therefore be applied on the full external boundary of the body.

3. Size effects in hardening: the bending of a beam

We will now compare the magnitude of the size effect predicted by the various higher-order plasticity theories. For this purpose, the micro-bending experiments of Stölken and Evans (1998) are taken as a prototypical case. In these experiments, nickel foils of different thicknesses were subjected to bending. As the thickness of these foils was reduced to a few microns, the bending moment generated in the test became significantly higher than that predicted by standard continuum mechanics. The authors also showed that this effect can be described by using a higher-order plasticity theory of the Fleck–Hutchinson 1997 type with linear hardening and a length scale on the order of a few microns. Below, we will perform similar analyses using each of the three higher-order theories and power-law hardening.

Following the analysis of Stölken and Evans (1998), a pure bending deformation is assumed, as well as a plane strain state in the x_3-direction, see Fig. 1. Furthermore, the deformation is assumed to be deep in the plastic range, such that elastic strains can be neglected. This means that the plastic strain tensor equals the total strain tensor, and for pure bending the nonvanishing components are given by

$$\varepsilon_{11} = \kappa x_2 \quad \varepsilon_{22} = -\kappa x_2 \tag{15}$$

where κ denotes the curvature of beam. The (plastic) strain gradient tensor of the Fleck–Hutchinson 1997 theory is also prescribed by the kinematics; the nonvanishing components read

$$\eta_{121} = \eta_{211} = \kappa \quad \eta_{112} = \eta_{222} = -\kappa \tag{16}$$

The above bending fields are assumed to be valid throughout the entire domain, including the upper and lower boundary. This seems to pose a problem for the two Fleck–Hutchinson theories, because it means that the (effective) plastic strain at this boundary is entirely prescribed and an essential boundary condition is thus set automatically. The higher-order tractions resulting from the bending field generally will not vanish and work will thus be done at the free boundary, which seems questionable from a physical point of view. A more realistic boundary condition would be the natural condition of vanishing higher-order tractions, which can be interpreted physically as the absence of any resistance to the glide of dislocations out of the material (Fleck and Hutchinson, 2001), but our freedom to set this boundary condition has been lost by assuming the total deformation field and neglecting elasticity. Note that the nonlocal model does not suffer from this difficulty, because its additional boundary condition is formulated in terms of the nonlocal effective plastic strain $\bar{\varepsilon}_p$, which is not prescribed by (15).

We shall demonstrate below that the inability of the Fleck–Hutchinson models to accommodate homogeneous natural boundary conditions in pure bending is only an apparent problem, introduced by the assumption of rigid-plastic behaviour. The correct overall size effect for these boundary conditions can still be extracted from a rigid-plastic analysis if the work done at the free boundary is taken into account properly.

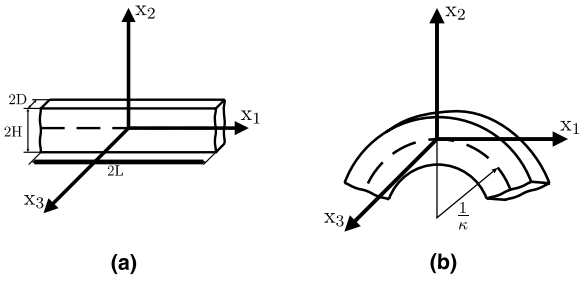

Fig. 1. Geometry of the bending specimen: (a) reference configuration; (b) bent specimen.

In order to show this, we will derive the size effect predicted by the elastoplastic solution for a particular case of the Fleck–Hutchinson 2001 theory and then take the limit of infinite elastic stiffness. The understanding gained from this analysis will be used in subsequent sections to determine the size effects predicted by the two Fleck–Hutchinson theories.

3.1. Calculation of bending moments for the Fleck–Hutchinson 2001 theory with linear hardening

The full, elastoplastic bending problem can be solved analytically for the Fleck–Hutchinson 2001 theory if we assume incompressible elastic behaviour and linear hardening plasticity. Closed-form expressions for the relevant fields are derived in Appendix A. Deep in the plastic range, the effective plastic strain is given in the top half of the specimen as a function of x_2 and κ by

$$\varepsilon_{\mathrm{p}} = \frac{2}{\sqrt{3}}\frac{E}{E+h}\kappa\left(x_2 - \lambda\frac{\sinh\frac{x_2}{\lambda}}{\cosh\frac{H}{\lambda}}\right) - \frac{\sigma_{\mathrm{y0}}}{E+h}\left(1 - \frac{\cosh\frac{H-x_2}{\lambda}}{\cosh\frac{H}{\lambda}}\right) \tag{17}$$

where σ_{y0} denotes the initial yield strength and the constant λ has been defined as

$$\lambda = l\sqrt{\frac{h}{E+h}} \tag{18}$$

The effective plastic strain, normalised by σ_{y0}/h, is plotted in Fig. 2 versus the normalised thickness co-ordinate x_2/H for a fixed curvature $\kappa = 0.1/H$ and for Young's moduli $E = 100\sigma_{\mathrm{y}}$ and $E = 1000\sigma_{\mathrm{y}}$. The internal length scale l equals $l = \frac{1}{2}H$ and a hardening modulus of $h = 20\ \sigma_{\mathrm{y0}}$ has been used. The dashed line in the diagram represents the rigid-plastic case, for which ε_{p} follows directly from the total strain fields as

$$\varepsilon_{\mathrm{p}} = \frac{2}{\sqrt{3}}\kappa x_2 \tag{19}$$

Note that this rigid-plastic solution is independent of the length scale and thus holds for gradient plasticity as well as for the standard rigid-plastic theory. Compared with this linear profile, the gradient-elastoplastic solutions clearly show a boundary layer near the top surface, in which the plastic strain is reduced in order to meet the higher-order boundary condition $t = hl^2\varepsilon_{\mathrm{p},2} = 0$. Inspection of the expression (17) reveals that the width of this boundary layer is set by the constant λ as defined above. For the smaller choice of value of E in Fig. 2(a) the constant λ is of the same order as the specimen thickness H and the effect of the boundary condition is noticeable even near the neutral axis (at $x_2/H = 0$). If Young's modulus is increased, however, λ decreases, the boundary layer becomes thinner and the effective plastic strain profile approaches that of the rigid-plastic case.

In order to comply with the imposed bending deformation, the reduced plastic strain in the boundary layer must be compensated by higher elastic strains, thus leading to higher stresses. This is illustrated in Fig. 2(b), where the axial stress distributions corresponding to the plastic strain distributions in Fig. 2(a) have been plotted. These profiles are given by (see Appendix A)

$$\sigma_{11} = \frac{2}{\sqrt{3}}\frac{E\sigma_{\mathrm{y0}}}{E+h}\left(1 - \frac{\cosh\frac{H-x_2}{\lambda}}{\cosh\frac{H}{\lambda}}\right) + \frac{4}{3}\frac{E}{E+h}\kappa\left(hx_2 + E\lambda\frac{\sinh\frac{x_2}{\lambda}}{\cosh\frac{H}{\lambda}}\right) \tag{20}$$

The dashed line again represents the rigid-plastic case, for which

$$\sigma_{11} = \frac{2}{\sqrt{3}}\sigma_{\mathrm{y0}} + \frac{4}{3}h\kappa x_2 \tag{21}$$

It is evident from Fig. 2 that the increased axial stress in the boundary layer leads to a higher bending moment in the strain gradient theory than in the standard theory; we shall show that this effect persists upon taking the limit of rigid-plastic behaviour. Consider the virtual work done by the bending moment M through the curvature variation $\delta\kappa$. This work can be written in terms of the standard and higher-order tractions as (cf. Fleck and Hutchinson, 2001)

$$\delta W = 2LM\delta\kappa = \int_S \left(T_i\delta u_i + t\delta\varepsilon_{\mathrm{p}}\right)\mathrm{d}S \tag{22}$$

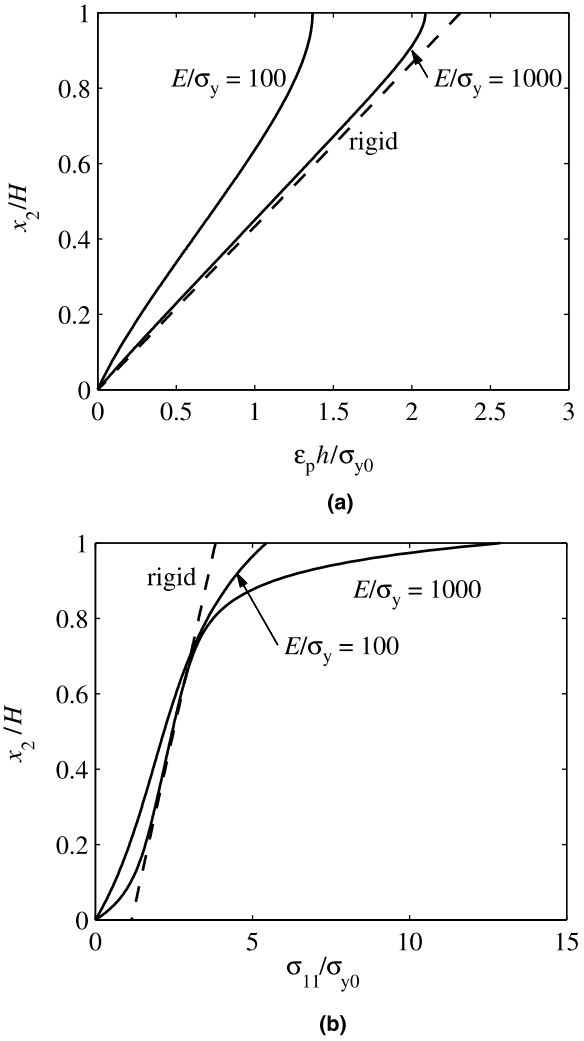

Fig. 2. Relevant fields obtained from the elastoplastic analysis for increasing Young's modulus: (a) effective plastic strain; (b) axial stress component. The dashed lines represent the rigid-plastic fields.

where $2L$ denotes the length of the considered beam section and S denotes its external surface. Now for the elastoplastic case the higher-order traction t vanishes everywhere on S, whereas the standard traction components T_i vanish on the top and bottom surfaces. The only remaining contribution to (22) comes from the traction across the cross-section of the specimen at both ends ($x_1 = \pm L$). Using $T_1 = \sigma_{11}$ and $\delta u_1 = L x_2 \delta\kappa$, we thus have for the bending moment

$$M = 4D \int_0^H x_2 \sigma_{11} \, \mathrm{d}x_2 \tag{23}$$

This establishes that, in the elastoplastic case, the standard expression in terms of stresses and the virtual work statement yield the same bending moment.

Evaluation of (23) for the stress field according to (20) gives

$$M = \frac{4}{\sqrt{3}} \frac{E\sigma_{y0}}{E+h} D H^2 \left(1 - 2\frac{\lambda^2}{H^2} \frac{\cosh\frac{H}{\lambda} - 1}{\cosh\frac{H}{\lambda}}\right) + \frac{16}{9} \frac{Eh}{E+h} \kappa D H^3 \left(1 + 3\frac{E}{h}\frac{\lambda^2}{H^2} - 3\frac{E}{h}\frac{\lambda^3}{H^3}\frac{\sinh\frac{H}{\lambda}}{\cosh\frac{H}{\lambda}}\right) \tag{24}$$

The factors outside the brackets are the usual contributions from standard, local elastoplasticity. The additional contributions depend upon λ and stem from the boundary layers at the centre and at the top and bottom of the specimen. Alternatively, the bending moment can be calculated via the internal virtual work.

The bending moment in the rigid-plastic limit can now be obtained from (24) by taking the limit $E \to \infty$. In this limit we have $\lambda \to 0$ and the width of the boundary layers thus vanishes (Fig. 2). Evaluation gives

$$M = \frac{4}{\sqrt{3}}\sigma_{y0}DH^2 + \frac{16}{9}h\kappa DH^3\left(1 + 3\frac{l^2}{H^2}\right) \tag{25}$$

The contribution involving the internal length l stems from the gradient influence. Although the thickness of the boundary layer tends to zero in the rigid-plastic limit, the boundary layer continues to deliver a finite contribution to the bending moment. As the thickness of the specimen, H, is diminished, the relative importance of this nonstandard term increases and the bending moment predicted by (25) diverges from that predicted by the standard theory. This is exactly the trend which is observed in experiments by Stölken and Evans (1998).

The expression (25) is uncontroversial because it has been obtained from the elastoplastic case, in which the influence of the higher-order boundary conditions is entirely clear. Our goal is now to demonstrate that this result can also be obtained directly from a much simpler, rigid-plastic analysis. It is immediately clear that substituting the rigid-plastic stress field (21) in expression (23) cannot yield the nonstandard contribution to the bending moment, because the length scale l does not appear in either of these relations. The bending moment predicted by the simple mechanical relation (23) thus does not show a size effect. To resolve this dichotomy, we revisit the virtual work statement (22) and note that at the top and bottom surface of the bending specimen the higher-order traction t no longer vanishes in the rigid-plastic analysis, but is prescribed by the plastic strain field. Taking into account this higher-order traction, as well as the symmetry and anti-symmetry properties of the relevant fields, the virtual external work performed by a curvature variation $\delta\kappa$ can be written for the rigid-plastic case as

$$\delta W = 8D\int_0^H T_1(x_2)\delta u_1(x_2)\mathrm{d}x_2 + 8LDt(H)\delta\varepsilon_{\mathrm{p}}(H) \tag{26}$$

Using the kinematic relations $\delta u_1 = Lx_2\delta\kappa$ and $\delta\varepsilon_{\mathrm{p}}(H) = 2/\sqrt{3}H\delta\kappa$ as well as $T_1 = \sigma_{11}$ and $t = \tau_2$, the bending moment can be extracted from this work statement as

$$M = 4D\int_0^H x_2\sigma_{11}\,\mathrm{d}x_2 + \frac{8}{\sqrt{3}}DH\tau_2(H) \tag{27}$$

The first term in (27) is the standard contribution of axial stresses, which also appears in the expression for the elastoplastic case (23). Substitution of the rigid-plastic stress field according to (21) in this term yields the bending moment which would be obtained for standard plasticity without any gradient influences. The second term, however, is nonstandard and gives rise to the size effect. It can easily be verified that the contribution of this term is identical to the nonstandard term in the bending moment as obtained by taking the rigid limit of the elastoplastic solution. Thus, the correct bending moment, given by (25), can be obtained from a rigid-plastic analysis by including the work done by the higher-order traction at the free boundary $x_2 = \pm H$ via relation (27). Equivalently, the correct bending moment can be obtained via the internal virtual work.

The above limiting process has the following physical interpretation. In the elastoplastic solution, the axial stress σ_{11} displays a concentration near the top surface of the specimen in order to meet the boundary condition imposed on the higher-order traction at this surface, recall Fig. 2. As the role of elastic strains is reduced by increasing Young's modulus, this concentration is limited to a smaller region but at the same time becomes more intense, in such a way that it continues to have a finite contribution to the overall bending moment and to the overall work, even in the rigid-plastic limit. In order to maintain the rigid-plastic fields (19) and (21), a higher-order traction t must exist at the free boundary. The internal virtual work associated with a curvature variation $\delta\kappa$ is exactly the same in the rigid-plastic case as in the rigid limit of the elastoplastic analysis. The extra external work which is required to maintain the plastic strain gradient is no longer introduced via the cross-section of the specimen, but through the top (and bottom) surfaces. The higher-order traction in the rigid-plastic solution can be taken to represent a boundary layer of vanishing thickness. Upon including

the contribution of this traction to the virtual work statement the correct bending moment is obtained; this correct value is identical to that obtained in the elastoplastic analysis upon taking the rigid-plastic limit.

It is concluded that a size effect is obtained in the simplified Fleck–Hutchinson 2001 theory despite the fact that for a constant hardening modulus h the consistency condition (11) contains only a second-order gradient of the effective plastic strain. The argument of Fleck et al. (1994) and Aifantis (1999) that a first-order gradient of plastic strain should enter this relation since all higher-order gradients vanish in the bending fields, does not hold here because it disregards the boundary contribution to the bending moment which we have identified above. As we will show below, the theory in its present form, without the first-order gradient contribution used by Aifantis (1999), shows a realistic size effect.

The expressions obtained here for the bending moment are specific to the case of the Fleck–Hutchinson 2001 theory with linear hardening. However, the underlying principle that the correct external loads can be obtained from a rigid-plastic analysis via a work statement can be applied more generally. Accordingly, we will use this principle in the remainder of this section not only for the Fleck–Hutchinson 2001 theory, but also for the Fleck–Hutchinson 1997 theory, and for nonlinear hardening. Note that the nonlocal plasticity theory does not require this re-interpretation of the bending moment, because homogeneous higher-order boundary conditions can be applied in it without any difficulty.

3.2. Fleck–Hutchinson 1997 strain gradient plasticity with power-law hardening

For the Fleck–Hutchinson 1997 elastoplastic flow theory it is convenient to compute the bending moment via the internal virtual work. Assuming a rigid-plastic response the internal virtual work reads $\delta W = \int_V \Sigma \delta E_p \, dV$, where Σ and E_p are the generalised equivalent stress and effective plastic strain as introduced in Section 2.1.

To proceed, we abandon the linear hardening law of the previous section and adopt the more realistic choice of power-law hardening in the remainder of this section. This allows the governing field equations to be homogeneous in stress and strain. For each of the theories the hardening relation is chosen such that it reduces to the classical Nadai power-law for a vanishing gradient influence, i.e. for $l = 0$. Note that this implies that the initial yield stress vanishes. In the Fleck–Hutchinson 1997 theory the hardening relation is generalised as $\sigma_y = CE_p^n$, where generally $0 < n < 1$ (Fleck and Hutchinson, 1997).

Following Stölken and Evans (1998) we neglect the influence of stretch gradients compared with rotation gradients for the bending problem. The generalised effective strain E_p is then given by

$$E_p = \frac{2}{\sqrt{3}} \kappa \sqrt{x_2^2 + \frac{1}{2} l^2} \tag{28}$$

Using this expression and the generalised equivalent stress $\Sigma = \sigma_y$, the bending moment can be extracted from the work statement in normalised form as

$$\frac{M}{M_0} = (n+2) \int_0^1 \left(\xi^2 + \frac{1}{2} \alpha^2 \right)^{\frac{n+1}{2}} d\xi \tag{29}$$

where $\xi \equiv x_2/H$, $\alpha \equiv l/H$ and

$$M_0 = \frac{4}{n+2} \left(\frac{2}{\sqrt{3}} \right)^{n+1} CDH^{n+2} \kappa^n \tag{30}$$

is the moment which results in classical plasticity (or for $l = 0$). It can easily be verified that the ratio given by (29) is always greater than unity for $l \neq 0$. For thicknesses which are large compared to the internal length scale l, that is for small α, M/M_0 is of order unity and the bending moment of the gradient theory reduces to that predicted by standard plasticity. As the thickness of the specimen is diminished (and α is thus increased), however, the second terms within brackets becomes more important and a strengthening effect is observed.

3.3. Fleck–Hutchinson 2001 strain gradient plasticity with power-law hardening

The generalised effective plastic strain of the Fleck–Hutchinson 2001 theory reads for the bending problem

$$E_{\mathrm{p}} = \frac{2}{\sqrt{3}}\kappa\sqrt{x_2^2 + l^2} \tag{31}$$

The hardening relation enters this theory via the hardening modulus h, which for power-law hardening reads $h = CnE_{\mathrm{p}}^{n-1}$.

It can be shown that the full and simplified versions of the Fleck–Hutchinson 2001 theory coincide for the bending problem. We can therefore use the consistency condition (11) to determine the equivalent stress rate. After integrating the result in time and obtaining the higher-order stress τ_2 in a similar manner, the bending moment can be evaluated using Eq. (27). In dimensionless form, the result reads, in terms of the dimensionless variables ξ and α as introduced above,

$$\frac{M}{M_0} = (n+2)\left[\int_0^1 \xi^2(\xi^2 - (n-2)\alpha^2)(\xi^2+\alpha^2)^{\frac{n-3}{2}}\mathrm{d}\xi + \alpha^2(1+\alpha^2)^{\frac{n-1}{2}}\right] \tag{32}$$

In the limit $\alpha \to 0$ this ratio clearly goes to unity again, whereas for large α (small H) it becomes large.

3.4. Nonlocal plasticity

The bending moment as predicted by the nonlocal plasticity formulation of Section 2.3 requires that we solve the partial differential equation (13) and boundary condition (14) for the bending problem. Upon inserting expression (19) for the effective plastic strain in (13) and noting that derivatives with respect to x_1 and x_3 must vanish, the partial differential equation reduces to an ordinary differential equation in terms of $\bar{\varepsilon}_{\mathrm{p}}$ for $0 < x_2 < H$, which together with homogeneous natural boundary conditions can be solved as

$$\bar{\varepsilon}_{\mathrm{p}} = \frac{2}{\sqrt{3}}\kappa\left(x_2 - l\frac{\cosh\frac{x_2}{l}}{\sinh\frac{H}{l}} + l\frac{\cosh\frac{H-x_2}{l}}{\sinh\frac{H}{l}}\right) \tag{33}$$

The solution in the bottom half of the specimen follows immediately by symmetry.

The stress distribution in the specimen can now be determined via the yield condition (12), in which the equality holds. For this purpose we make the choice for the yield stress as $\sigma_{\mathrm{y}} = C\varepsilon_{\mathrm{p}}^{n-m}\bar{\varepsilon}_{\mathrm{p}}^{m}$, with $0 < n < 1$ and $-n \leqslant m \leqslant n$. This form is inspired by the multiplicative character of the damaged yield stress in the original model (Engelen et al., 1999, 2003). The parameter m determines the relative influences of the local and nonlocal effective plastic strains on the yield stress. For $m = 0$ note that σ_{y} depends solely upon ε_{p} and the local theory is thus retrieved; for $m = n$, on the other hand, σ_{y} depends solely upon $\bar{\varepsilon}_{\mathrm{p}}$ and the multiplicative influence of both strain measures is lost. For any value of m, it can be seen directly that standard Nadai hardening is retrieved when the internal length is set to zero and the nonlocal and local strain fields thus coincide.

Substitution of the ε_{p} and $\bar{\varepsilon}_{\mathrm{p}}$ fields in the above hardening law allows one to compute the equivalent stress and the axial stress σ_{11} as well as, via (23), the corresponding bending moment. The result reads, normalised with respect to the classical result,

$$\frac{M}{M_0} = (n+2)\int_0^1 \xi^{n-m+1}\left(\xi - \alpha\frac{\cosh\frac{\xi}{\alpha}}{\sinh\frac{1}{\alpha}} + \alpha\frac{\cosh\frac{1-\xi}{\alpha}}{\sinh\frac{1}{\alpha}}\right)^m \mathrm{d}\xi \tag{34}$$

In the limit $\alpha \to 0$ this ratio approaches unity as for the other theories. But for larger α (smaller thicknesses) either a strengthening or a weakening effect is predicted depending on the value of the parameter m, as we shall see below.

3.5. Comparison of predicted size effects for a beam in bending

Fig. 3 shows the normalised bending moments M/M_0 predicted for each of the higher-order plasticity theories as given by expressions (29), (32) and (34) as a function of the ratio H/l (or $1/\alpha$). The integrals in the

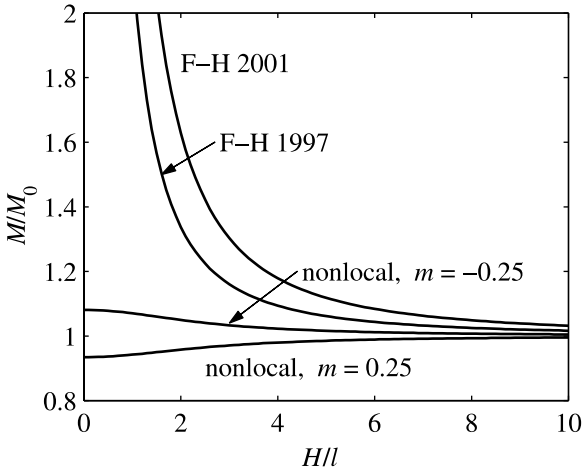

Fig. 3. Comparison of the normalised bending moments predicted by the three higher-order plasticity theories as a function of the thickness of the specimen relative to the internal length l. A hardening exponent of $n = 0.5$ has been used.

respective expressions for M/M_0 have been evaluated numerically. A value of $n = 0.5$ has been used for the hardening exponent. A change in the hardening exponent changes the quantitative results, but not the qualitative picture. Two values were used for the parameter m in the nonlocal theory: $m = 0.25$ and $m = -0.25$. As can be seen from the diagram, this parameter has a significant influence upon the predicted trend. For $m = 0.25$, and in fact for all positive m, the theory predicts a weakening effect for small H/l. A strengthening effect can be obtained by setting $m < 0$, as is illustrated by the curve for $m = -0.25$. However, this effect remains rather small compared with experimental observations: the elevation in M/M_0 is less than 10% for $m = -0.25$, whereas strengthening by a factor of up to 5 was observed in the experiments (Stölken and Evans, 1998). The two Fleck–Hutchinson theories predict a much stronger strengthening effect, and are in much better agreement with the experimental results of Stölken and Evans.

It is remarkable how closely the two Fleck–Hutchinson theories match, even if no attempt has been made to correlate the length scales of the two theories. The reduction of the full strain gradient theory (Fleck–Hutchinson 1997) to the simpler 2001 Fleck–Hutchinson theory seems to be quite acceptable for this boundary value problem.

4. Prediction of the higher-order theories of the transition to softening and localisation behaviour

Having analysed the size effect in hardening for the three higher-order plasticity formulations, the transition to material softening and subsequent localisation is now considered. Many materials display an overall softening behaviour after a certain amount of plastic deformation. For example, metals may soften due to the initiation, growth and coalescence of voids, resulting in the localisation of deformation and eventually in failure.

It is well known that material softening within a local continuum plasticity description may result in the loss of well-posedness of the governing equations (Benallal et al., 1989), and homogeneous boundary value problems then have an infinite number of solutions. For the case of inhomogeneous problems instantaneous failure is predicted within a band of vanishing width without any energy dissipation. Numerical solutions are limited in capturing this discontinuous solution by their finite spatial resolution and therefore show an extreme sensitivity to the numerical discretisation. Higher-order formulations may restore the well-posedness of the boundary value problem. As a result, deformation bands of finite width are obtained, in which a finite amount of energy is dissipated (Bažant et al., 1984, see for example; Pijaudier-Cabot and Bažant, 1987; de Borst and Mühlhaus, 1992; Engelen et al., 2003).

In homogeneous problems without imperfections, localised solutions appear as bifurcations of the homogeneous solution. We shall consider the bifurcation problem next in a one-dimensional setting. The starting

point is a bar under uniform tensile straining. At each state of this uniform solution, an incremental solution is sought of the harmonic form $\dot{\varepsilon} = \hat{\varepsilon}\exp(\mathrm{i}kx)$, where $\hat{\varepsilon}$ denotes the complex amplitude of the harmonic perturbation and k its wave number. This harmonic field is substituted into the rate equilibrium equations, assuming a state of plastic loading on the entire domain (Hill's linear comparison solid assumption, see Hill (1958)). The rate equilibrium equations are then examined in order to determine the wave numbers for which the harmonic incremental solution exists.

In a local continuum (as in classical plasticity), no harmonic incremental solutions exist in the elastic regime as well as in the hardening plasticity regime. At the onset of softening, however, a continuous spectrum of wave numbers k is found for which the above harmonic form is a solution of the incremental equilibrium problem, including that which represents a vanishing wavelength (i.e. $k \to \infty$). This reflects the ill-posedness of the problem and the pathological localisation which results from it (Peerlings et al., 2002). The desired behaviour of the higher-order plasticity theories considered here is bifurcation into a finite number of solutions, each with a finite wave number.

The ability of the Fleck and Hutchinson 1997 and 2001 theories and the nonlocal theory of Engelen et al. (1999, 2003) to handle material softening is now explored by considering the bifurcation of a bar under uniform tensile straining.

4.1. Fleck–Hutchinson 1997 elastoplastic strain gradient plasticity theory

Consider first the prediction of bifurcation by the Fleck–Hutchinson 1997 elastoplastic strain gradient plasticity theory. We consider a uniform reference solution with $\eta = \eta_{\mathrm{p}} = \tau \equiv 0$ in the reference state. This implies that the generalised effective plastic strain equals $E_{\mathrm{p}} = \varepsilon_{\mathrm{p}}$ and the generalised equivalent stress $\Sigma = \sigma$; we also have $\dot{\Sigma} = \dot{\sigma}$ and it follows from normality that $\dot{E}_{\mathrm{p}} = \dot{\varepsilon}_{\mathrm{p}}$. Using these relations, the flow rules which govern the evolution of ε_{p} and η_{p} can be written as (cf. Fleck and Hutchinson, 1997)

$$\dot{\varepsilon}_{\mathrm{p}} = \frac{\dot{\Sigma}}{h(E_{\mathrm{p}})}\frac{\sigma}{\Sigma} = \frac{\dot{\sigma}}{h(\varepsilon_{\mathrm{p}})} \quad \dot{\eta}_{\mathrm{p}} = \frac{\dot{\Sigma}}{h(E_{\mathrm{p}})}\frac{\tau}{\Sigma} = 0 \tag{35}$$

where $h(E_{\mathrm{p}}) = \mathrm{d}\sigma_{\mathrm{y}}/\mathrm{d}E_{\mathrm{p}}$ describes the current hardening/softening behaviour in the material. The second of the above relations tells us that the rate of plastic strain gradient vanishes. Combining the first with Hooke's law and the higher-order rate equilibrium equation and substituting for the assumed harmonic form of $\dot{\varepsilon}$ yields

$$\mathrm{i}kE\left(\frac{h}{E+h} + k^2 l^2\right)\hat{\varepsilon}\exp(\mathrm{i}kx) = 0 \tag{36}$$

Apart from the trivial solution $\hat{\varepsilon} = 0$, the above equation has only one real solution as long as the tangent h is positive: $k = 0$. This solution represents a continued uniform deformation. Once h becomes negative, however, a second solution appears

$$k = \frac{1}{l}\sqrt{\frac{-h}{E+h}} \tag{37}$$

This means that at each uniform reference state in the softening regime the possibility of bifurcation into a harmonic solution exists. This harmonic solution of the homogeneous, linear comparison solid problem corresponds to a localised solution of the underlying nonlinear equations in inhomogeneous problems. The wave number k given by relation (37) remains finite, which means that the corresponding wavelength $2\pi/k$ is always positive. Full, nonlinear numerical solutions have been performed for similar higher-order theories and confirm that the pathological solution $2\pi/k = 0$ does not exist (Peerlings et al., 2002). The above result demonstrates that the Fleck–Hutchinson 1997 theory shows the desired localisation behaviour at and beyond the transition from hardening to softening.

It is worth noting that the higher-order contribution in (36), and therefore the regularisation, comes from the elastic part of the constitutive modelling. This is best seen from relation $(35)_2$, which states that the plastic strain gradient does not come into play. Accordingly, although so far no distinction has been made between elastic and plastic length scales, the internal length l in (37) should be interpreted as the internal length

associated with the elastic response of the material. This analysis is confirmed by Rolshoven (2003), who has shown that the width of the plastic localisation band depends mainly on the elastic length scale, with only a secondary influence of the plastic length scale.

4.2. Fleck–Hutchinson 2001 strain gradient plasticity

The generalised effective plastic strain of the Fleck and Hutchinson 2001 theory (Fleck and Hutchinson, 2001) coincides with ε_p in the uniform reference solution. Combining the one-dimensional version of the consistency relation (11), the incremental form of Hooke's law and the rate equilibrium equation $\dot{\sigma}_{,x} = 0$ allows one to derive the nonlinear eigenvalue equation

$$\mathrm{i}kE\frac{h(1+k^2l^2)}{E+h(1+k^2l^2)}\hat{\varepsilon}\exp(\mathrm{i}kx) = 0 \tag{38}$$

For $h > 0$ this relation again has only the trivial solution $k = 0$. At the transition from hardening to softening, $h = 0$, however, Eq. (38) is trivially satisfied and any harmonic wave number k is allowed. This indicates that pathological localisation at the peak strength is not prevented by the Fleck and Hutchinson 2001 theory. Beyond the peak strength, in the softening regime, we have $h < 0$ and (38) has again only the trivial solution. Thus, in contrast to the earlier Fleck–Hutchinson theory, no wavelength can be identified for which the uniform reference solution may bifurcate into a harmonic incremental solution. Although these observations do not provide irrefutable proof with respect to the nonlinear case, they do cast serious doubt upon the ability of the theory to handle localisation events in an adequate fashion.

It should be mentioned here that gradient plasticity models with a structure which is very similar to that of the present one have been used with some degree of success to regularise localisation in the softening regime (Aifantis, 1984; de Borst and Mühlhaus, 1992). In these theories the higher-order contribution to the hardening law is added to the local contribution rather than subtracted from it. In our analysis this would result in a minus sign in front of the k^2l^2 in (38). The resulting equation does have a nontrivial solution $k = 1/l$ in the softening regime and a nonuniform incremental solution with a finite wavelength can thus be obtained. However, this solution is also available in the hardening plastic regime (i.e. for $h > 0$), which suggests that nonuniform solutions can occur even before the peak load. Indeed, it seems that previous applications of these theories have been limited to situations where the plastic softening sets in immediately at the elastic limit, without any prior hardening. In connection to this, it has been argued by Mühlhaus and Aifantis (1991) and Fleck and Hutchinson (2001) that such a formulation cannot be obtained from a work statement. Mühlhaus and Aifantis (1991) suggested to repair this shortcoming by adding a fourth-order gradient contribution to it. While interesting from a theoretical viewpoint, this is not a very attractive option in terms of numerical implementation, because it would impose stringent continuity requirements on the interpolation functions used in the spatial discretisation of the problem.

4.3. Nonlocal plasticity

In the nonlocal plasticity model of Section 2.3 the nonstandard plastic strain measure $\bar{\varepsilon}_p$ is governed by Eq. (13). This measure enters the constitutive response via the hardening/softening law, which can be rewritten in the present case as

$$\dot{\sigma} = h(\varepsilon_p, \bar{\varepsilon}_p)\dot{\varepsilon}_p + \bar{h}(\varepsilon_p, \bar{\varepsilon}_p)\dot{\bar{\varepsilon}}_p \tag{39}$$

where $h(\varepsilon_p, \bar{\varepsilon}_p) = \partial\sigma_y/\partial\varepsilon_p$ and $\bar{h}(\varepsilon_p, \bar{\varepsilon}_p) = \partial\sigma_y/\partial\bar{\varepsilon}_p$. Combining these relations with rate equilibrium and substituting the harmonic form of $\dot{\varepsilon}$ gives

$$\mathrm{i}kE\frac{h(1+k^2l^2)+\bar{h}}{(E+h)(1+k^2l^2)+\bar{h}}\hat{\varepsilon}\mathrm{e}^{\mathrm{i}kx} = 0 \tag{40}$$

in which the arguments of h and $\bar{h}$ have been dropped for brevity.

Whether or not this equation has nontrivial solutions k depends upon the current values of the hardening moduli h and $\bar{h}$. These also determine whether the incremental response is hardening or softening. For uniform straining, we have $\bar{\varepsilon}_p = \varepsilon_p$ and the stress rate can thus be written as $\dot{\sigma} = (h + \bar{h})\dot{\varepsilon}_p$. This relation shows that a hardening behaviour is observed when the sum of the two moduli is positive while softening occurs when this sum becomes negative. In the plasticity-damage formulation of Engelen et al. (1999, 2003) the local contribution h is always positive, whereas $\bar{h}$ is always negative. Initially, their sum will usually be positive and a hardening incremental response is thus observed. It can easily be seen that Eq. (40) only has the trivial solution $k = 0$ when the sum of the two moduli is positive. At some stage of the uniform straining process, however, the balance between h and $\bar{h}$ may change and their sum may change sign, thus resulting in a transition to a softening response. Exactly at the peak, that is for $h + \bar{h} = 0$, the trivial, uniform solution is still the only one, but when the sum of the two moduli becomes negative, a second, nontrivial solution of (40) exists, and is given by

$$k = \frac{1}{l}\sqrt{-\frac{h+\bar{h}}{h}} \tag{41}$$

It is concluded that the nonlocal plasticity formulation allows for a transition from hardening to softening, and within the softening regime it correctly predicts a localisation band of finite width.

4.4. Comparison of the predicted wavelengths in the softening regime

In order to compare the localisation behaviour of the three plasticity theories, we need to assume a specific form of the hardening/softening relations featuring in them. The choice of these relations was motivated by the plasticity-damage theory of Engelen et al. (1999, 2003), as this theory was developed to describe softening and localisation. Accordingly, we assume the following law for the nonlocal plasticity theory:

$$\sigma_y = \sigma_{y0}\left(1 + \frac{C}{\sigma_{y0}}\varepsilon_p^n\right)\left(1 - \frac{\bar{\varepsilon}_p}{\varepsilon_c}\right) \tag{42}$$

This relation can be regarded as a combination of power-law hardening (in terms of the local plastic strain ε_p) and a linear degradation which depends upon the nonlocal plastic strain $\bar{\varepsilon}_p$ (cf. Engelen et al., 1999, 2003). When the nonlocal strain attains the critical value ε_c, the yield strength vanishes and failure is obtained. The local and nonlocal hardening moduli $h(\varepsilon_p, \bar{\varepsilon}_p)$ and $\bar{h}(\varepsilon_p, \bar{\varepsilon}_p)$ used within the nonlocal plasticity theory follow by straightforward differentiation of (42). It can easily be verified that the resulting expression for h is indeed always positive and $\bar{h}$ is always negative, as assumed in the previous section.

In the Fleck–Hutchinson 1997 theory, the yield stress σ_y depends upon the generalised effective plastic strain E_p, cf. Section 2.1. For this theory we assume the following hardening/softening law:

$$\sigma_y = \sigma_{y0}\left(1 + \frac{C}{\sigma_{y0}}E_p^n\right)\left(1 - \frac{E_p}{\varepsilon_c}\right) \tag{43}$$

and the tangent modulus again follows by differentiation. The resulting expression is also used for the Fleck–Hutchinson 2001 theory.

For the case of uniform plastic straining, with $\bar{\varepsilon}_p = E_p = \varepsilon_p$, the three constitutive theories give identical hardening/softening behaviours along the primary loading path. The axial stress versus plastic strain curve is shown in Fig. 4 for the choice $C = 4\sigma_{y0}$, $n = 0.5$ and $\varepsilon_c = 1$; these values are adopted in the remainder of this section. It is clear from Fig. 4 that the material displays a hardening response up to a plastic strain of $\varepsilon_p = \frac{1}{4}\varepsilon_c$. At this value of plastic strain, the tangent to the curve is horizontal and a transition to softening behaviour occurs. Softening continues until complete failure occurs at $\varepsilon_p = \varepsilon_c$.

The nontrivial wavelengths $2\pi/k$, normalised by the length scale l, are plotted in Fig. 5 as a function of normalised plastic strain $\varepsilon_p/\varepsilon_c$ for each of the higher-order theories. A value of $E = 100\sigma_{y0}$ is adopted for Young's modulus. In the Fleck–Hutchinson 2001 theory, the incremental solution can take all wavelengths at the peak load (i.e. at $\varepsilon_p/\varepsilon_c = \frac{1}{4}$). Beyond this peak load, no solution exists for a finite wavelength, as was shown in Section 4.2. In contrast, the other two theories give a finite wavelength within the softening regime. At $\varepsilon_p/\varepsilon_c = \frac{1}{4}$ both curves have a vertical asymptote, indicating that at the peak load only a uniform incremental solution

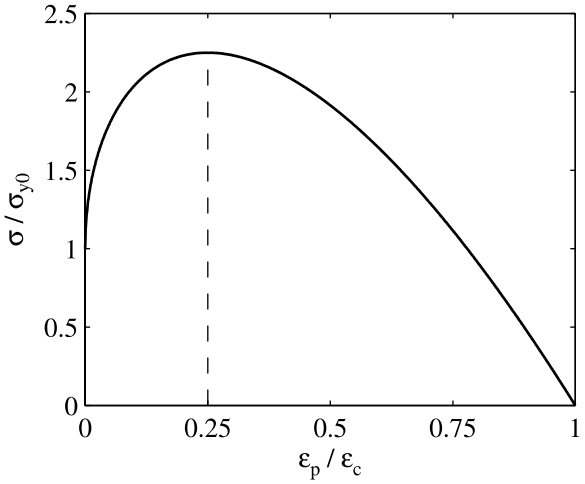

Fig. 4. Hardening/softening behaviour for uniform straining as used for all three theories in the localisation study.

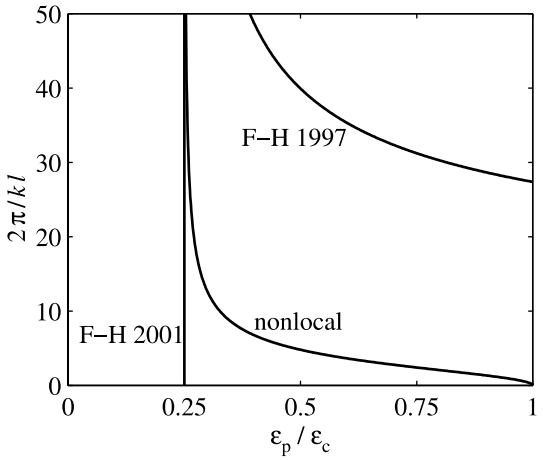

Fig. 5. Normalised wavelength $2\pi/kl$ of the localised incremental solution vs the normalised plastic strain $\varepsilon_p/\varepsilon_c$ in the uniform reference state for the three higher-order theories.

exists. Beyond the peak, however, a finite wavelength is obtained, and this wavelength decreases with increasing reference strain for both theories. In the Fleck–Hutchinson 1997 theory a finite wavelength is obtained at failure (i.e. at $\varepsilon_p/\varepsilon_c = 1$), whereas the wavelength goes to zero in the nonlocal theory. The latter could be an advantage in situations where a gradual transition from a diffuse degradation mechanism to a discrete crack is desired, see e.g. Simone et al. (2003). Apart from this qualitative difference, the wavelength predicted by the Fleck–Hutchinson 1997 theory is—for the same value of the internal length l—much higher than that predicted by the nonlocal theory. This difference is due to the appearance of Young's modulus in the wavelength of the Fleck–Hutchinson theory; for higher ratios E/σ_{y0} than that used here the difference becomes even more pronounced. However, it can easily be compensated for by choosing a smaller length scale in the Fleck–Hutchinson theory. This is quite acceptable since the relevant length scale in the theory is associated with the elastic behaviour (cf. Fleck and Hutchinson, 1997).

5. Concluding remarks

The relative performance of three prototypical higher-order plasticity theories has been explored. Two extreme test cases have been considered: the prediction of size effects in the hardening regime and the ability

Table 1
Summary of the evaluation of the three theories in terms of size effect predictions and localisation behaviour

Theory	Size effect	Localisation
Fleck–Hutchinson 1997	++	+
Fleck–Hutchinson 2001	++	−
Nonlocal	−	++

to remove the pathological localisation behaviour exhibited by standard plasticity theory within the softening regime. Our findings are summarised in Table 1, in which ++ denotes an excellent performance, + denotes a satisfactory performance, and − indicates shortcomings or at least serious concerns.

Each of the three theories have been developed with either size effects or localisation in mind: the two Fleck–Hutchinson theories were developed to describe size effects, whereas the nonlocal theory was originally aimed at handling softening and localisation in a reliable and meaningful way. It is therefore not surprising that these theories perform well in the corresponding prototype problems. Extraction of the physically relevant size effect for a beam in bending for the Fleck–Hutchinson theories, however, requires a careful treatment of the stress state near the free boundary, as was illustrated in Section 3.

As summarised in Table 1, the Fleck–Hutchinson 1997 theory can predict finite-sized shear bands and degradation zones in the softening regime in addition to giving realistic size effects in hardening. This is of particular relevance to problems where localisation and size effects become important at the same time, e.g. in problems of large plastic deformations leading to damage in the manufacture of small components. The ability to handle localisation stems from the presence of a gradient influence in the elastic part of the constitutive theory rather than from plastic strain gradients. Furthermore, unlike the nonlocal theory, the localisation width predicted by the Fleck–Hutchinson 1997 theory does not vanish at complete failure. This may not be a problem in most applications, but it is less desirable in computational approaches which use a so-called continuum–discontinuum transition (e.g. Simone et al., 2003).

The other two theories are incapable of describing both phenomena adequately. The Fleck–Hutchinson 2001 theory in unable to remove the pathological behaviour of standard plasticity when passing from the hardening to the softening regime. As indicated in Section 4.2, we believe that this conclusion holds for a wider category of weakly nonlocal gradient theories, although acceptable results may be obtained in very specific cases. The nonlocal plasticity theory which was modelled after the plasticity-damage framework of Engelen et al. (1999, 2003) gives a size effect in the bending problem, but depending upon parameter values this effect is either too small or in the wrong direction (weakening instead of the experimentally observed strengthening). Here also we believe that a similar weakness is present in other nonlocal plasticity formulations; additional work is needed to substantiate this, however.

Acknowledgements

This research was carried out under project number ME.97037 in the framework of the strategic research programme of the Netherlands Institute for Metals Research in the Netherlands (NIMR, URL: www.nimr.nl). Part of this work was performed during a stay of the first author at the Department of Engineering of the University of Cambridge with Professor Norman A. Fleck. Hospitality and financial support from the European Communities TMR programme 'Spatio-temporal instabilities in deformation and fracture: mechanics, materials science and nonlinear physics aspects', project reference FMRX960062, are gratefully acknowledged.

Appendix A. Analytical solution for the elastoplastic bending problem

For the Fleck–Hutchinson 2001 theory, the solution for the elastoplastic bending problem can be obtained in closed form if a constant hardening modulus h is assumed and the elastic behaviour is assumed to be incompressible. We will do the analysis here for the upper half of the beam ($x_2 \geqslant 0$) and assuming positive curvature for ease of notation; the lower half can then easily be obtained by symmetry arguments.

For an incompressible elastoplastic material the total strain rate can be written in the plastic regime as

$$\dot{\varepsilon}_{ij} = \frac{3}{2E}\dot{s}_{ij} + \frac{3}{2}\dot{\varepsilon}_{\mathrm{p}}\frac{s_{ij}}{\sigma_{\mathrm{e}}} \tag{A.1}$$

where E denotes Young's modulus and s_{ij} the deviatoric stresses. Setting these strain rate components equal to the imposed deformation according to (15) and using the definition of the equivalent stress σ_{e} gives $s_{33} = 0$, $s_{11} = -s_{22} = \sigma_{\mathrm{e}}/\sqrt{3}$ and

$$\frac{1}{2}\sqrt{3}\left(\frac{\dot{\sigma}_{\mathrm{e}}}{E} + \dot{\varepsilon}_{\mathrm{p}}\right) = \dot{\kappa}x_2 \tag{A.2}$$

For the beam-bending problem it can be shown that the full and simplified versions of the Fleck–Hutchinson 2001 theory coincide. Upon substituting (11) for the effective stress rate the above equation becomes

$$\dot{\varepsilon}_{\mathrm{p}} - \lambda^2\dot{\varepsilon}_{\mathrm{p},22} = \frac{2}{\sqrt{3}}\frac{E}{E+h}\dot{\kappa}x_2 \tag{A.3}$$

where the constant λ is

$$\lambda = l\sqrt{\frac{h}{E+h}} \tag{A.4}$$

It is useful to adopt x_2 and κ as the independent variables and rewrite the problem in terms of them by using $\partial/\partial t = \dot{\kappa}\partial/\partial\kappa$:

$$\frac{\partial}{\partial\kappa}\left(\varepsilon_{\mathrm{p}} - \lambda^2\varepsilon_{\mathrm{p},22}\right) = \frac{2}{\sqrt{3}}\frac{E}{E+h}x_2 \tag{A.5}$$

The general solution of this equation can be written as

$$\varepsilon_{\mathrm{p}}(x_2,\kappa) = \frac{2}{\sqrt{3}}\frac{E}{E+h}\kappa x_2 + f_{\mathrm{c}}(\kappa)\cosh\frac{x_2}{\lambda} + f_{\mathrm{s}}(\kappa)\sinh\frac{x_2}{\lambda} + g(x_2) \tag{A.6}$$

In this expression, $f_{\mathrm{c}}(\kappa)$, $f_{\mathrm{s}}(\kappa)$ and $g(x_2)$ are still arbitrary functions, which must be determined from the boundary data.

Eq. (A.5) and its general solution (A.6) are valid in that part of the beam which has already entered the plastic regime. This elastoplastic domain has been sketched in the x_2–κ space as a shaded area in Fig. A.1, and is sub-divided into two sub-domains II and III, as shown. At sufficiently low values of κ the beam is

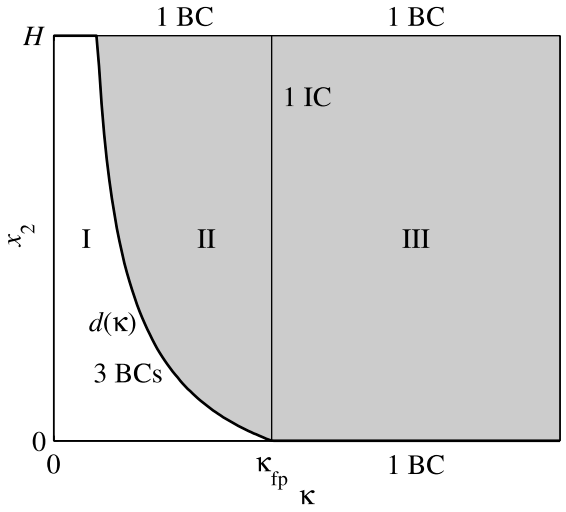

Fig. A.1. Solution domain in x_2–κ space for the elastoplastic bending problem.

elastic, and this domain is labelled I in Fig. A.1. It will be shown below that the elastic–plastic boundary, i.e. the boundary between sub-regions I and II, meets the neutral axis at a finite value of curvature κ, as suggested in the figure. This value of κ indicates the onset of fully plastic behaviour and is denoted κ_{fp}. First we will concentrate on the sub-domain II, for which the plastic domain is sandwiched between the top of the beam ($x_2 = H$) and the elastic–plastic boundary. The position of this internal boundary at a given curvature is not known a priori, but follows from the solution. The function $d(\kappa)$ indicates the height of this boundary and must be determined together with $f_{\mathrm{c}}(\kappa)$, $f_{\mathrm{s}}(\kappa)$ and $g(x_2)$ from the boundary data. Four boundary conditions are thus needed: one at the top surface and three at the elastic–plastic boundary (see the figure).

Since the top surface is free, it is natural to set the higher-order traction to zero here:

$$hl^2\varepsilon_{\mathrm{p},2}(H,\kappa) = 0 \tag{A.7}$$

At the elastic–plastic boundary we have

$$\varepsilon_{\mathrm{p}}(d(\kappa),\kappa) = 0 \tag{A.8}$$

$$hl^2\varepsilon_{\mathrm{p},2}(d(\kappa),\kappa) = 0 \tag{A.9}$$

$$\sigma_{\mathrm{y0}} + h\varepsilon_{\mathrm{p}}(d(\kappa),\kappa) - hl^2\varepsilon_{\mathrm{p},22}(d(\kappa),\kappa) = \frac{2}{\sqrt{3}}E\kappa d(\kappa) \tag{A.10}$$

with σ_{y0} the initial yield stress. The second of these relations expresses vanishing higher-order traction on the elastic–plastic boundary; the first and last ensure continuity of plastic strain and equivalent stress across this boundary. The functions $f_{\mathrm{c}}(\kappa)$, $f_{\mathrm{s}}(\kappa)$ and $g(x_2)$ can be solved in terms of $d(\kappa)$ by substituting the general solution (A.6) into the relations (A.7), (A.9) and (A.10). Eq. (A.6) then gives

$$\varepsilon_{\mathrm{p}} = \frac{2}{\sqrt{3}}\frac{E}{E+h}\kappa\left(x_2 - \lambda\frac{\cosh\frac{x_2-d(\kappa)}{\lambda}}{\sinh\frac{H-d(\kappa)}{\lambda}} + \lambda\frac{\cosh\frac{H-x_2}{\lambda}}{\sinh\frac{H-d(\kappa)}{\lambda}}\right) - \frac{\sigma_{\mathrm{y0}}}{E+h} \tag{A.11}$$

An implicit relation for the position of the elastic–plastic boundary, $d(\kappa)$, is determined by the condition (A.8), with a behaviour of the form sketched in Fig. A.1. The curvature κ_{fp} for which $d(\kappa)$ becomes zero is determined by setting $x_2 = d = \varepsilon_{\mathrm{p}} = 0$ in (A.11) to give

$$\kappa_{\mathrm{fp}} = \frac{1}{2}\sqrt{3}\frac{\sigma_{\mathrm{y0}}}{E\lambda}\frac{\sinh\frac{H}{\lambda}}{\cosh\frac{H}{\lambda}-1} \tag{A.12}$$

Now consider curvatures which exceed the value κ_{fp}; this is denoted sub-domain III in Fig. A.1. The bottom boundary of the plastic zone is fixed at $x_2 = 0$ with $\varepsilon_{\mathrm{p}} = 0$ there. The boundary condition at $x_2 = H$ remains unchanged. Recall that the governing partial differential equation, Eq. (A.5), constitutes an initial value problem in κ as a time-like parameter, and a boundary value problem in the spatial dimension x_2. The initial condition for sub-domain III is provided by the solution of sub-domain II, as given by (A.11), at $\kappa = \kappa_{\mathrm{fp}}$. The general solution to (A.6) can be determined for $\kappa > \kappa_{\mathrm{fp}}$ as

$$\varepsilon_{\mathrm{p}} = \frac{2}{\sqrt{3}}\frac{E}{E+h}\kappa\left(x_2 - \lambda\frac{\sinh\frac{x_2}{\lambda}}{\cosh\frac{H}{\lambda}}\right) - \frac{\sigma_{\mathrm{y0}}}{E+h}\left(1 - \frac{\cosh\frac{H-x_2}{\lambda}}{\cosh\frac{H}{\lambda}}\right) \tag{A.13}$$

The solutions (A.11) and (A.13) for $\varepsilon_{\mathrm{p}}(x_2,\kappa)$ in sub-domains II and III, respectively, are plotted in Fig. A.2. In this diagram, the effective plastic strain, normalised by σ_{y0}/h, is plotted horizontally versus the vertical relative co-ordinate x_2/H. This solution was obtained for the choice $l = \frac{1}{2}H$, a Young's modulus of $E = 100\sigma_{\mathrm{y0}}$ and a hardening modulus $h = 20\sigma_{\mathrm{y0}}$. Curves are plotted for $\kappa = 0.02/H$, for $\kappa = \kappa_{\mathrm{fp}} \approx 0.04/H$ and for $\kappa = 0.1/H$. For the first curve $\kappa < \kappa_{\mathrm{fp}}$ and the elastic–plastic boundary is therefore located above the neutral axis at $x_2 > 0$; at this boundary the higher-order traction vanishes and so the gradient of ε_{p} vanishes. At $\kappa = \kappa_{\mathrm{fp}}$, the elastic–plastic boundary touches the neutral axis and at $\kappa = 0.1/H > \kappa_{\mathrm{fp}}$, the plastic zone extends across the full cross-section of the beam. In the latter case, on the neutral axis, $x_2 = 0$, a higher-order traction exists and the gradient of ε_{p} is finite. However, ε_{p} is zero at $x_2 = 0$ and so this traction does no work.

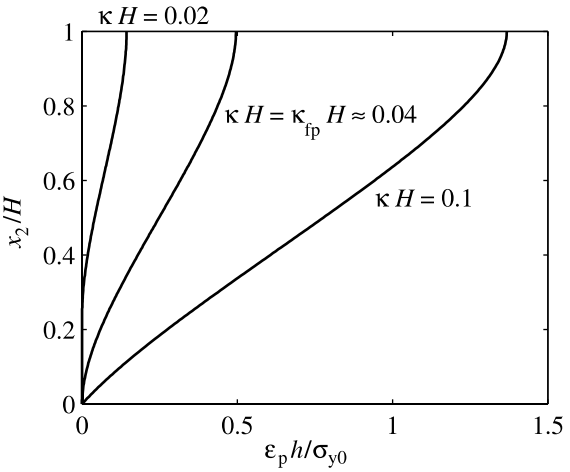

Fig. A.2. Effective plastic strain distribution in the top half of the beam for increasing curvature κ.

The equivalent stress in each of the plastic domains II and III is obtained by integration of (11) and by substitution of the effective plastic strain distributions obtained above, to give

$$\sigma_e = \frac{E\sigma_{y0}}{E+h} + \frac{2}{\sqrt{3}}\frac{E}{E+h}\kappa\left(hx_2 + E\lambda\frac{\cosh\frac{x_2-d(\kappa)}{\lambda}}{\sinh\frac{H-d(\kappa)}{\lambda}} - E\lambda\frac{\cosh\frac{H-x_2}{\lambda}}{\sinh\frac{H-d(\kappa)}{\lambda}}\right) \quad \text{for } \kappa \leqslant \kappa_{fp} \tag{A.14}$$

and

$$\sigma_e = \frac{E\sigma_{y0}}{E+h}\left(1 - \frac{\cosh\frac{H-x_2}{\lambda}}{\cosh\frac{H}{\lambda}}\right) + \frac{2}{\sqrt{3}}\frac{E}{E+h}\kappa\left(hx_2 + E\lambda\frac{\sinh\frac{x_2}{\lambda}}{\cosh\frac{H}{\lambda}}\right) \quad \text{for } \kappa > \kappa_{fp} \tag{A.15}$$

The axial stress σ_{11} is obtained from the above expressions via $\sigma_{11} = 2s_{11} = 2\sigma_e/\sqrt{3}$. The only nonvanishing component of the higher-order stress vector is $\tau_2 = hl^2\varepsilon_{p,2}$.

References

Aifantis, E.C., 1984. On the microstructural origin of certain inelastic models. J. Eng. Mater. 106, 326–330.
Aifantis, E.C., 1999. Strain gradient interpretation of size effects. Int. J. Fract. 95, 299–314.
Bažant, Z.P., 2000. Size effect. Int. J. Solids Struct. 37, 69–80.
Bažant, Z.P., Belytschko, T., Chang, T.P., 1984. Continuum theory for strain-softening. J. Eng. Mech. 110, 1666–1692.
Begley, M.R., Hutchinson, J.W., 1998. The mechanics of size-dependent indentation. J. Mech. Phys. Solids 46, 2049–2068.
Benallal, A., Billardon, R., Geymonat, G., 1989. Some mathematical aspects of the damage softening rate problem. In: Mazars, J., Bažant, Z.P. (Eds.), Cracking and Damage, Strain Localization and Size Effect. Proc. France–US Workshop. Elsevier, London, pp. 247–258.
Coleman, B.D., Hodgdon, M.L., 1985. On shear bands in ductile materials. Arch. Rat. Mech. Anal. 90, 219–247.
de Borst, R., Mühlhaus, H.-B., 1992. Gradient-dependent plasticity: Formulation and algorithmic aspects. Int. J. Numer. Methods Eng. 35, 521–539.
de Borst, R., Sluys, L.J., Mühlhaus, H.-B., Pamin, J., 1993. Fundamental issues in finite element analysis of localization of deformation. Eng. Comput. 10, 99–121.
Engelen, R.A.B., Geers, M.G.D., Baaijens, F.P.T., 1999. Gradient-enhanced plasticity formulations based on the dependency of the yield stress on a nonlocal field variable. In: Proc. European Conference on Computational Mechanics. Munich, Germany, on CD-ROM.
Engelen, R.A.B., Geers, M.G.D., Baaijens, F.P.T., 2003. Nonlocal implicit gradient-enhanced elasto-plasticity for the modelling of softening behaviour. Int. J. Plasticity 19, 403–433.
Fleck, N.A., Hutchinson, J.W., 1993. A phenomenological theory for strain gradient effects in plasticity. J. Mech. Phys. Solids 41, 1825–1857.
Fleck, N.A., Hutchinson, J.W., 1997. Strain gradient plasticity. Adv. Appl. Mech. 33, 295–361.
Fleck, N.A., Hutchinson, J.W., 1998. A discussion of strain gradient plasticity theories, and application to shear bands. In: de Borst, R., van der Giessen, E. (Eds.), Material Instabilities in Solids, IUTAM Symposium, Delft, June 1997. John Wiley & Sons, Chichester, UK, pp. 507–520.
Fleck, N.A., Hutchinson, J.W., 2001. A reformulation of strain gradient plasticity. J. Mech. Phys. Solids 49, 2245–2271.

Fleck, N.A., Muller, G.M., Ashby, M.F., Hutchinson, J.W., 1994. Strain gradient plasticity: theory and experiment. Acta Metall. Mater. 42, 475–487.

Geers, M.G.D., Ubachs, R.L.J.M., Engelen, R.A.B., 2003. Strongly nonlocal gradient-enhanced finite strain elastoplasticity. Int. J. Numer. Methods Eng. 56, 2039–2068.

Hill, R., 1958. A general theory of uniqueness and stability in elastic–plastic solids. J. Mech. Phys. Solids 6, 236–249.

Leblond, J.B., Perrin, G., Devaux, J., 1994. Bifurcation effects in ductile metals with damage delocalisation. J. Appl. Mech. 61, 236–242.

Ma, Q., Clarke, D.R., 1995. Size dependent hardness of silver single crystals. J. Mater. Res. 10, 853–863.

Mindlin, R.D., 1964. Micro-structure in linear elasticity. Arch. Rat. Mech. Anal. 16, 51–78.

Mindlin, R.D., 1965. Second gradient of strain and surface tension in linear elasticity. Int. J. Solids Struct. 1, 417–438.

Mühlhaus, H.-B., Aifantis, E.C., 1991. A variational principle for gradient plasticity. Int. J. Solids Struct. 28, 845–857.

Needleman, A., Tvergaard, V., 1998. Dynamic crack growth in a nonlocal progressively cavitating solid. Eur. J. Mech. A/Solids 17, 421–438.

Peerlings, R.H.J., de Borst, R., Brekelmans, W.A.M., de Vree, J.H.P., 1996. Gradient-enhanced damage for quasi-brittle materials. Int. J. Numer. Methods Eng. 39, 3391–3403.

Peerlings, R.H.J., de Borst, R., Brekelmans, W.A.M., Geers, M.G.D., 2002. Localisation issues in local and nonlocal continuum approaches to fracture. Eur. J. Mech. A/Solids 21, 175–189.

Peerlings, R.H.J., Geers, M.G.D., de Borst, R., Brekelmans, W.A.M., 2001. A critical comparison of nonlocal and gradient-enhanced softening continua. Int. J. Solids Struct. 38, 7723–7746.

Pijaudier-Cabot, G., Bažant, Z.P., 1987. Nonlocal damage theory. J. Eng. Mech. 113, 1512–1533.

Polizzotto, C., Borino, G., Fuschi, P., 1998. A thermodynamically consistent formulation of nonlocal and gradient plasticity. Mech. Res. Comm. 25, 75–82.

Poole, W.J., Ashby, M.F., Fleck, N.A., 1996. Micro-hardness of annealed and work-hardened copper polycrystals. Scr. Mater. 34, 559–564.

Rolshoven, S., 2003. Nonlocal plasticity models for localized failure. Ph.D. thesis, Ecole Polytechnique Fédérale de Lausanne, Lausanne, Switzerland.

Shu, J.Y., van der Giessen, E., Needleman, A., 2001. Boundary layers in constrained plastic flow: comparison of nonlocal and discrete dislocation plasticity. J. Mech. Phys. Solids 49, 1361–1395.

Simone, A., Wells, G.N., Sluys, L.J., 2003. From continuous to discontinuous failure in a gradient-enhanced continuum damage model. Comput. Methods Appl. Mech. Eng. 192, 4581–4607.

Stölken, J.S., Evans, A.G., 1998. A microbend test method for measuring the plasticity length scale. Acta Mater. 46, 5109–5115.

Strömberg, L., Ristinmaa, M., 1996. FE-formulation of a nonlocal plasticity theory. Comput. Methods Appl. Mech. Eng. 136, 127–144.

Toupin, R.A., 1962. Elastic materials with couple stresses. Arch. Rat. Mech. Anal. 11, 385–414.